Hollow fibre membrane-based liquid desiccant humidity control for controlled environment agriculture

Lefers, Ryan M.; Srivatsa Bettahalli, N.m.; Fedoroff, Nina V.; Ghaffour, Noreddine; Davies, Philip A.; Nunes, Suzana P.; Leiknes, Torove

DOI:
10.1016/j.biosystemseng.2019.04.010

Hollow Fibre Membrane-based Liquid Desiccant Humidity Control for Controlled Environment Agriculture

AUTHORS COPY

Citation: Biosystems Engineering, Volume 183, 2019, Pages 47-57, ISSN 1537-5110, https://doi.org/10.1016/j.biosystemseng.2019.04.010.

Ryan Lefers [a *], N.M. Srivatsa Bettahalli [a,b], Nina Fedoroff [c], Noreddine Ghaffour [a], Philip A. Davies [d], Suzana P. Nunes [e], TorOve Leiknes [a]

[a] King Abdullah University of Science and Technology (KAUST), Water Desalination & Reuse Center (WDRC), Biological and Environmental Science and Engineering Division (BESE), Thuwal 23955-6900, Saudi Arabia

[b] Advanced Membranes and Porous Materials Center (AMPMC), Physical Science and Engineering Division (PSE) at KAUST

[c] Evan Pugh Professor Emerita, Penn State University, University Park, PA 16802, USA

[d] School of Engineering, University of Birmingham, Birmingham, UK

[e] King Abdullah University of Science and Technology (KAUST), Biological and Environmental Science and Engineering Division (BESE), Thuwal 23955-6900, Saudi Arabia

* Corresponding author: Ryan Lefers

Email address: ryan.lefers@kaust.edu.sa

Research highlights

- Liquid desiccant in triple bore hollow fibre membrane
- Humidity successfully controlled at levels desirable for plant cultivation
- Dehumidification rate varies dynamically in response to plant transpiration rate
- Average membrane dehumidification permeance of 0.26-0.31 g m^{-2} h^{-1} Pa^{-1}

Abstract

Humidity control is an important factor affecting the overall sustainability, productivity, and energy efficiency of controlled environment agriculture. Liquid desiccants offer the potential for pinpoint control of humidity levels in controlled environments. In the present work, a dehumidification processes utilizing liquid desiccants pumped through the lumens of triple-bore PVDF hollow fibre membranes is implemented in a bench scale controlled environment agriculture system. Hydrophobic hollow fibre membranes were combined into an array and placed near the crops. Concentrated magnesium chloride liquid desiccant solution with a low vapour pressure was pumped through the hollow fibre lumens. The dehumidification permeance rate responded dynamically to the changing transpiration rate of the plants, as influenced by changes in environmental factors such as light, temperature, and vapour pressure. The dehumidification permeance rate increased from an average of 0.26 to 0.31 g m^{-2} h^{-1} Pa^{-1} as the velocity of the liquid desiccant through the hollow fibres increased from 0.023 to 0.081 m s^{-1}. Humidity levels were targeted to be maintained within a range of 70-90% relative humidity at 23 °C. The membrane-based liquid desiccant system was demonstrated to successfully control humidity within a bench-scale controlled environment agricultural setup.

45 Keywords: Controlled environment agriculture; humidity control; hydrophobic hollow fibre
46 membrane; dehumidification; liquid desiccant; sustainable agriculture

47 **Graphical Abstract**

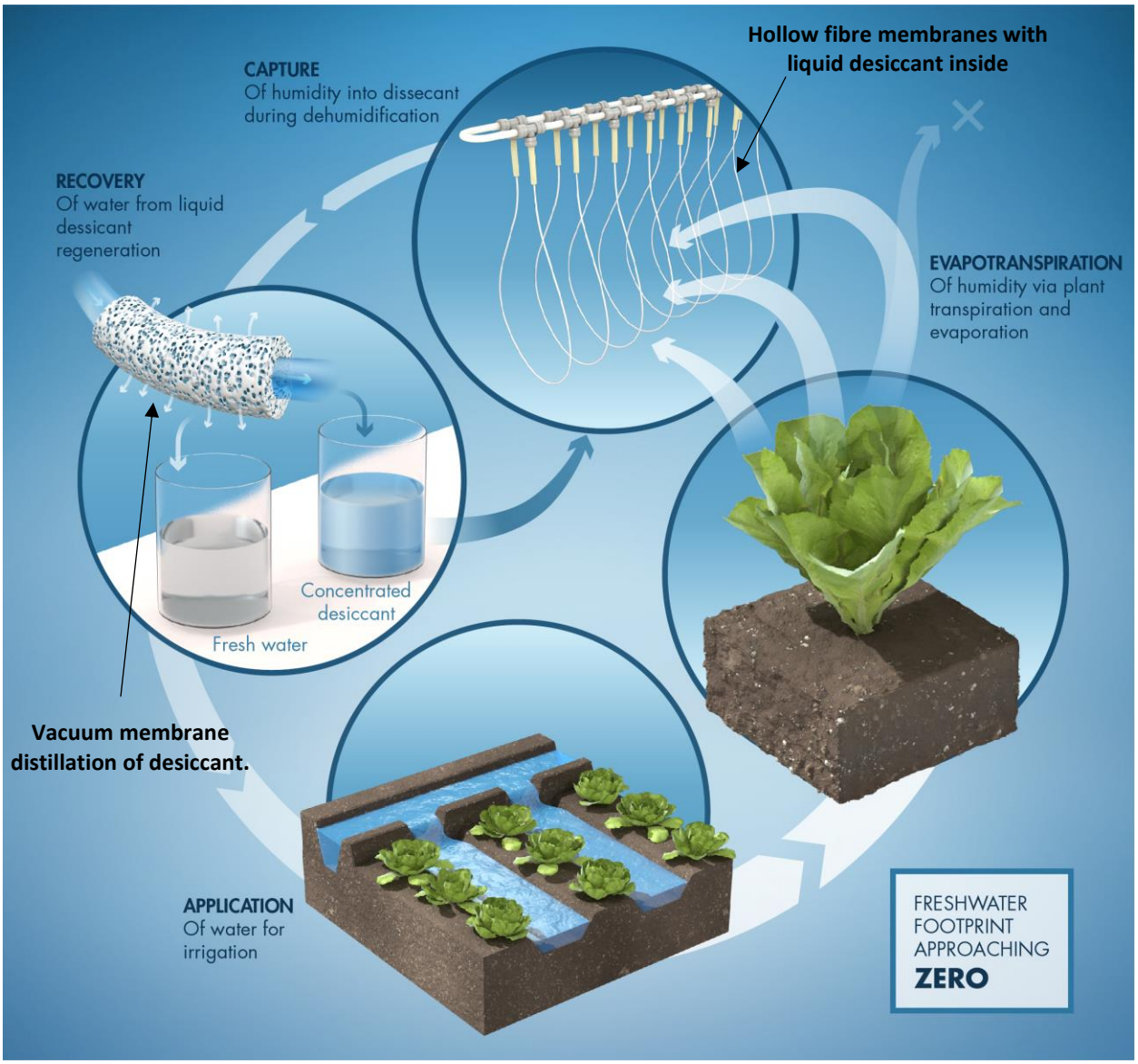

48
49 *Water and liquid desiccant cycles when utilizing the proposed hollow fibre membrane-based liquid desiccant humidity*
50 *control system for controlled environment agriculture.*

51

1 Introduction

The proper management of water for agriculture is of critical concern to diverse spheres of influence in the world community (Lefers, Maliva, & Missimer, 2015). The withdrawal of water to grow food constitutes around 70% of the total global water use, a relationship known as the global food-water nexus (FAO, 2016). The total amount of water required to grow a unit of food is known as the crop water footprint (Mekonnen & Hoekstra, 2011). Indoor agriculture, also referred to as controlled environment agriculture (CEA), offers the potential to greatly reduce the water footprint of crops while also increasing produce quality. Irrigation water use/loss due to surface runoff, deep percolation, weed transpiration, and soil evaporation can be reduced or eliminated indoors using modern cultivation technologies such as recycling hydroponics and aquaponics. The production water footprint in such systems can nearly be limited to water used by crop transpiration.

In addition to water savings, humidity control in CEA is also important from the perspective of crop performance. Too low humidity levels can lead to excessive plant transpiration, stunting, wilting, disease, and crop injury. When humidity levels become too high, plant transpiration and internal plant nutrient transport can be slowed, pollination of flowering/fruiting crops can be impacted and the risk of plant diseases and fungus can increase (Bakker, 1991; Hand, 1988; Hickman, 2014; Resh, 2013) . With these risks in mind, humidity management in the controlled environment can lead to better overall plant health and increased crop productivity.

Humidity control in CEA is usually accomplished by a release of humid indoor air to the outdoor environment when levels indoors are above desired (Campen, Bot, & de Zwart, 2003; Hickman, 2014; Resh, 2013). The release of temperature-conditioned indoor air to the outdoor environment is of concern as it relates to energy use. In hot or cold climates, when humid indoor air is released to the environment and replaced by drier outdoor air, the incoming air must be conditioned (heated or cooled) to match crop needs (typically targeted at 16-28° C) (Resh, 2013). The heating and/or cooling of the incoming dry air consumes energy. In addition to heating energy and water savings, carbon dioxide enrichment for increased crop production would be better achieved in closed systems without the need for air exchange in the climate control system.

As alternatives to ventilation of humid air from the CEA system (CEAS), dew-point condensers and desiccant systems can be used to dehumidify air in situ. Desiccant systems differ from common dew-point condenser systems in that the indoor air does not need to reach its dew point temperature for humidity removal to take place. Desiccant contactors function based upon vapour pressure difference rather than dew point condensation due to air saturation. Therefore, desiccant systems offer the potential for humidity regulation in indoor air at ambient temperatures (Dean et al., 2012; Dijkink, Tomassen, Willemsen, & van Doorn, 2004; Hwang, Radermacher, Al Alili, & Kubo, 2008; Kassem, 2013; Khan, 1994; Kozubal, Woods, Burch, Boranian, & Merrigan, 2011; Lowenstein, 2008; Mohammad, Mat, Sulaiman, Sopian, & Al-Abidi, 2013; Zhang, Yin, & Zhang, 2016; Zhang, Zhang, & Xu, 2016). Desiccants may be attractive for humidity removal over refrigeration-based dew point systems in that they offer the potential for

92 a lower grid-energy footprint. Although desiccant regeneration requires energy input, the
93 opportunity exists to make use of thermal energy sources such as solar energy or industrial waste
94 heat (Kozubal et al., 2011; Lowenstein, 2008) and renewable electricity-generating sources such
95 as solar photovoltaics and wind turbines to support pumps, fans, control systems, etc.

96 Both solid and liquid desiccants can be used, however, liquid desiccants offer operational
97 flexibility for pumping and storage. Liquid desiccants can absorb water vapour directly or through
98 a membrane contactor. The use of membrane contactors in liquid desiccant based
99 dehumidification systems has been evaluated by a number of authors (Abdel-Salam, Ge, &
100 Simonson, 2013; Bergero & Chiari, 2010; Das & Jain, 2013; Isetti, Nannei, & Magrini, 1997; Keniar,
101 Ghali, & Ghaddar, 2015; Kneifel et al., 2006; Zhang, 2011; Zhang, Yin, et al., 2016; Zhang, et al.,
102 2016). Membrane contactors offer a number of advantages for use with liquid desiccant
103 dehumidification systems. Membrane contactors can greatly increase the surface area per unit
104 volume for mass transfer above what would be realized in an open pan or trench type desiccant
105 system. As compared to a packed-bed type direct-contactor system, membrane contactors offer
106 protection for both the desiccant solution and the surrounding environment. For the desiccant,
107 the membrane provides a barrier against pollutants such as dust and airborne particulates.
108 Common liquid desiccants include concentrated salts such as lithium chloride, lithium bromide,
109 magnesium chloride and calcium chloride (Davies & Knowles, 2006; Lychnos, Fletcher, & Davies,
110 2010). These desiccant salt solutions are corrosive for many common metals used as equipment
111 materials of construction (Lowenstein, 2008). The salt solutions may also damage plant tissue if
112 direct contact takes place (spills, aerosols, etc.). By keeping the solution separated behind a

nano-porous hydrophobic membrane, both the risks of corrosion and contact can be eliminated. Moreover, the membrane interface allows for independent operation of liquid and gas phases (Albrecht et al., 2005; Rajat & Jain, 2015; Kneifel et al., 2006). In spite of the many advantages, potential drawbacks to application of membranes in liquid desiccant cycles are the added mass transport resistance of the membrane and the potential for additional cost compared to a direct-contact system.

Compared to flat or tubular membrane contactors, and to direct-contact systems, the use of hollow fibres with liquid desiccants for dehumidification applications is attractive because of the high surface area provided per unit volume (Gabelman & Hwang, 1999). In addition, the number of pores per unit volume of hollow fibres can offer faster, more efficient moisture transport if leakage can be prevented. Single-bore hollow fibres have been used successfully with liquid desiccants for dehumidification by other authors (Dijkink et al., 2004; Kneifel et al., 2006; Zhang, Yin, et al., 2016; Zhang et al., 2016). A device utilizing triple-bore hollow fibre membranes was proposed for dehumidification based on a liquid desiccant solution pumped through polyvinylidene fluoride (PVDF) hollow fibres (Bettahalli, Lefers, Fedoroff, Leiknes, & Nunes, 2016). The triple-bore structure was preferred over the single-bore structure because it offered additional mechanical stability, allowing the fibres to be used in the open indoor environment rather than in a protected module. In this study, the triple-bore hollow fibre PVDF membranes are integrated into a bench-scale controlled environment agricultural setup (CEAS) for humidity control.

The aim of this study was to evaluate the use of the triple bore hollow fibre array liquid desiccant system for controlling the humidity levels within a CEAS. Of special interest was to see if the system would be able to maintain humidity levels within a set target range, similar to those desired for production agriculture in a closed system. For this work, a target range was selected between 70-90% relative humidity at ~22-23°C, with a vapour pressure deficit >0.25 kPa, and a humidity deficit of ~2.0 g m^{-3} to 6.5 g m^{-3} (Bakker, 1991; Hand, 1988; Hickman, 2014; Resh, 2013). The target range selected for this work is not meant to represent the range that would be selected in commercial practice by all growers for all crops, rather, the range was selected to provide a general reference window to show the potential for the liquid desiccant system to keep indoor humidity levels within a generally desired range. This work demonstrates utilizing liquid desiccants with triple-bore hollow fibre membranes for humidity control in a CEAS. This work also demonstrates the potential for a closed water cycle within the CEAS based upon fresh water recovery from the liquid desiccants. Such a system has significant potential for applications such as space travel, laboratories for specialized studies or developments, and for water-limited locations around the globe.

2 Materials and methods

2.1 Bench scale controlled environment agriculture setup

A bench-scale box "greenhouse" CEAS was designed and fabricated for use under laboratory conditions. A bench-scale size of system was necessary to show the performance of the hollow fibre based dehumidification system while having control over influencing variables such as can

be achieved in a laboratory environment. Figure 1 shows the bench-scale setup. The interior dimensions of the box were 50 cm x 50 cm x 50 cm. These dimensions were chosen to allow the growing of real crops in a closed controlled environment of a minimum size. The greenhouse was placed on a bench in the Water Desalination and Reuse Center laboratory at KAUST. The greenhouse was equipped with a fan for air circulation to maintain a uniform distribution of humidity and temperature within the controlled environment (Sunon model KD1208PTS1, 12V, 2.6W). A small-scale Miracle-Gro Aerogarden 3SL hydroponics unit equipped with a full spectrum Compact Fluorescent Light (CFL) grow light was placed inside the CEAS and used for plant production. This hydroponics unit with associated lighting is representative on a very small scale of similar systems deployed at large scale in vertical farms, also called plant factories. The crops grown during the experimental trials included one plant each of cherry tomato, parsley and lettuce (varieties: mighty mini cherry tomato, curly parsley, and deer tongue lettuce, all sourced from www.aerogarden.com.) The CFL irradiation intensity was measured by a Spectroradiometer ILT950 (International Light Technologies, www.intl-lighttech.com). The distance from the CFL to the top of the crop was kept constant as the crops grew at approximately 10 cm, providing a radiation intensity of approximately 0.15 MJ m^{-2} h^{-1} at this distance. A logging temperature/humidity sensor (Testo 175H1 model, ±0.4 °C ±2% RH) was placed inside the CEAS to record instantaneous temperature and humidity at 10 min intervals. A hot wire anemometer (Testo 435-4 multifunction meter equipped with model no. 0635 1535 thermal velocity probe) was used to determine the average air circulation speed near the surface of the plant leaves. As the fan speed was constant and did not vary over time, the air velocity was only recorded at the beginning and end of the experiment.

The root zone in the hydroponics unit was aerated via an air pump using air from the closed bench-scale greenhouse environment. The air bubbles in the hydroponics system were released back into the indoor environment through the coir media supporting plant roots. The air pump operated when the CFL light was on and stopped operation when the CFL light was off. The aeration system could have provided additional humidity to the closed indoor environment in addition to the transpired water vapour from cultivated crops.

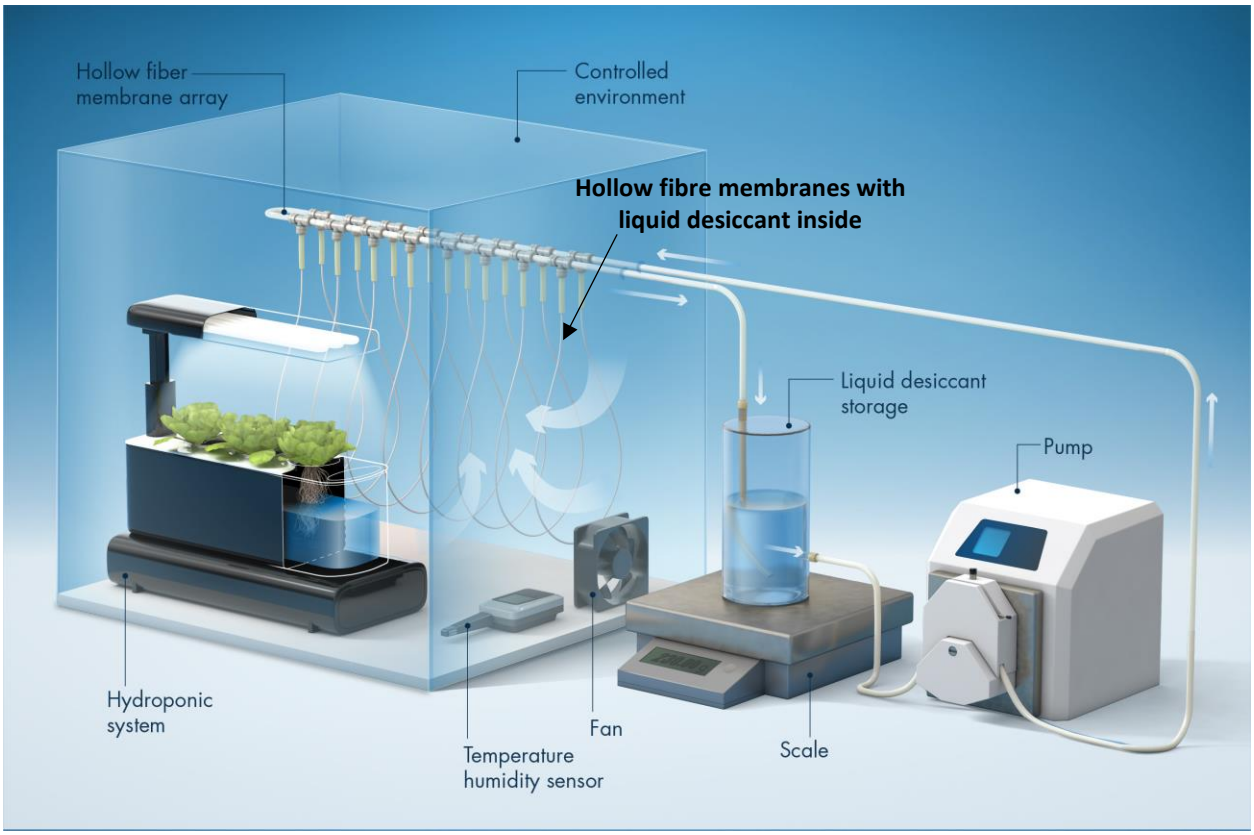

Figure 1 Bench-scale greenhouse setup process schematic.

2.2 **Hollow fibre membranes**

An array of hydrophobic PVDF hollow fibre membranes was positioned adjacent to the side of the hydroponics unit for dehumidification. The hollow fibres were manufactured in the lab using

186 the techniques as described in Bettahalli et al., (2016). Scanning electron microscope (SEM)
187 images of hollow fibres are shown in Figure 2. A desiccant solution was pumped at a fixed flow
188 rate through the lumens of an array of eight hollow fibres. The length of each exposed fibre varied
189 from 52.5 cm to 59 cm, with a total combined length of 448 cm. The outer and inner diameters
190 of the hollow fibres were 1.82 mm and 0.78 mm (3 total inner diameters due to triple bore),
191 respectively. The total surface area of the hollow fibre membranes used was ~0.0256 m^2. The
192 liquid entry point (LEP) value was measured via a Porolux 1000 with Porefil (perfluoroether)
193 (surface tension 16 mN m^{-1}, according to the Porolux manual). The LEP as measured was 1.52
194 bar, which corresponds to a pore size of 420 nm. A mean pore size of 390 nm was measured
195 using capillary flow porosimetry with Porefil as the wetting liquid.

196 The hollow fibres were installed to operate in a parallel array in a U-shape as shown in Figure 1.
197 Liquid desiccant entered the fibres at one end from a pump and tubing connected to the
198 desiccant tank. Humidity was then absorbed across the entire length of the fibres as the desiccant
199 passed through. The desiccant exited the other end of the hollow fibres into tubing that returned
200 the desiccant to the storage tank.

201

Cross section	Outer wall
	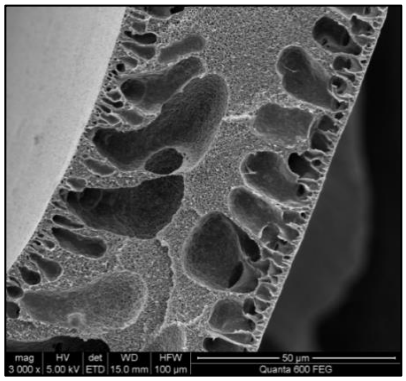

Figure 2 SEM images of triple-bore PVDF hollow fibres manufactured in the lab. (Bettahalli et al., 2016)

2.3 **Liquid desiccant humidity control system**

Relative humidity and temperature in the bench-scale greenhouse fluctuated based upon crop transpiration, heat input from the CFL, heat gained/lost from the CEAS walls, and heat and humidity added/removed by the liquid desiccant as pumped through the hollow fibre membrane array. The liquid desiccant pump used in the experiment was a Masterflex® L/S model no. 7523-80 peristaltic pump, size 0.1-600 RPM at 0.1 horsepower. The desiccant solution was pumped through the lumens of hollow fibres at three velocities in three separate experimental trials: 2.3 cm s^{-1}, 4.7 cm s^{-1} and 8.1 cm s^{-1}. The desiccant temperature was warmed or cooled inside the CEAS and/or in the lab room, as the walls of the hollow fibres were in direct contact with the CEAS air and the walls of the glass liquid desiccant storage container and tubing were in direct contact with the lab room air. The temperatures of the desiccant immediately before entry into and after exit from the hollow fibre membrane array were logged using inline PT100 platinum

resistance sensors (3 mm diameter x 150 mm length) attached to PT-104 screw terminal adapters (PP660) and connected into a Pico Technology PT-104 PT100 data logger. Desiccant temperature was recorded every 10 min. The pressure of the desiccant solution at the entry to the hollow fibre array was monitored using a Keller brand Mano LEO 1, with a range of 0 to 31 bar absolute pressure (www.keller-druck.ch). The desiccant storage container was placed on an electronic balance (Mettler Toledo model MS4002S, ±0.01 g) for recording the weight at 10 min intervals. The dehumidification flux (kg m^{-2} h^{-1}) of the desiccant was measured by recording the change in solution weight over time and dividing by the total membrane surface area.

Magnesium chloride solution was used as the liquid desiccant for all dehumidification experiments. Magnesium chloride was chosen because of its relative lower cost compared to other salts and because it is effective at the relative humidity ranges expected in the controlled agriculture environment (~70-90% relative humidity). The concentration of magnesium chloride by weight decreased over time during dehumidification, as water was added to the desiccant solution via humidity capture. Refractive index, used to determine the concentration of the desiccant before and after experimental runs, was checked using a Reichert Technologies Brix/RI-Check Refractometer. The refractometer was calibrated daily using distilled fresh water.

For each experimental trial, the same bulk desiccant solution was used, however, the solution was regenerated (water removed) between trials via vacuum membrane distillation using the methods described in Lefers et. al. (2018). Membrane distillation (MD) is a thermally driven process that utilizes a hydrophobic, micro-porous membrane as a contactor to achieve separation by liquid-vapour equilibrium. The driving force for the MD process is the partial

vapour pressure difference maintained at the two sides of the membrane. The hot feed solution is brought into contact with the membrane which allows only the water vapour to go through its dry pores and get condensed on the cold side which is maintained by a cooling medium (inside the module) or by applying a low environment vacuum to create a vapour pressure difference (outside the module). The latter configuration, i.e. vacuum MD (VMD), is used in this study. MD produces very high water quality with typical rejection above 99.95% for a wide range of feed water used, including hypersaline feeds (Xu et. al., 2016). A detailed description of the VMD concept and its main advantages and operational challenges can be found elsewhere (Alsaadi et. al., 2014; Alsaadi et. al., 2018; Fortunato et al., 2018). In the present work, the liquid desiccant was heated to a temperature of 30° C and vacuum was applied to achieve an absolute pressure of 3 mbar on the air side of the membrane using the setup described in Lefers et. al. (2018). The recovered fresh water distillate from the VMD process was reused for irrigation in the hydroponics unit. The distillate was weighed and added to the bench-scale hydroponics unit as make-up water at the start of each experimental trial to account for water used by plants for transpiration. A Mettler Toledo model ML3002E weighing scale was used to measure the water weight. Nutrients for the hydroponic solution were also weighed and added to the bench-scale system in sufficient amounts to meet plant requirements. To account for water retained within plant tissue or lost due to potential leaks in the controlled environment (not transpired), a small amount of additional fresh water was required to top off water levels within the hydroponics system at the full level. This additional fresh water was also weighed before being added to the system, such that the total mass of the mixed water and nutrient solution added at the end of each experimental trial was recorded.

2.4 **Crop transpiration equations**

Evapotranspiration was both measured directly and estimated from theoretical equations. Evapotranspiration was measured directly by weighing the amount of water required to refill the hydroponics setup at the end of each experimental run, as previously described. While this provided a direct measurement of the water use at the end of each experimental run (~100 hours), it did not provide an estimate of instantaneous evapotranspiration. Therefore, a theoretical equation was used to estimate instantaneous evapotranspiration in mm h^{-1}. The Stanghellini equation was chosen for the bench-scale greenhouse setup as it is recommended to estimate evapotranspiration in medium and high technology greenhouses (Ilahi, 2009; Villarreal-Guerrero et al., 2012). Important sensor-measured parameters for input into the Stanghellini equation included the light irradiation intensity, temperature, humidity, and air speed.

The evapotranspiration was estimated using the Stanghellini equation (Equation 1), with input parameters as defined in Table 1.

$$ET_p = 2\,LAI\,\frac{1}{\lambda}\left(\frac{s(R_n-G)+K_t\left(\frac{VPD\rho C_p}{r_R}\right)}{s+\gamma\left(1+{}^{r_c}/_{r_a}\right)}\right) \quad (1)$$

Table 1 Parameters used in the Stanghellini equation to calculate evapotranspiration.

Constant	Value	Description
LAI	2.88	Leaf area index, $m^2\ m^{-2}$
λ	2.45	Latent heat of vaporization, MJ kg^{-1}
G	0	Soil heat flux, suggested at 0 (Stanghellini, 1987; Vuscovich, 2001), MJ $m^{-2}\,h^{-1}$
K_t	3600	Unit conversion factor to acquire mm h^{-1} of ET, s h^{-1}

C_p	0.001013	Specific heat of air, MJ kg^{-1} °C^{-1}
γ	0.06735	Psychrometric constant at 101.325 kPa atmospheric pressure, kPa °C^{-1}
r_c	240 or 1900	Canopy internal resistance, estimated at 240 with grow light on and 1900 with grow light off from (Villarreal-Guerrero et al., 2012), s m^{-1}
K_c	0.6	Selected crop coefficient, (Casanova, Messing, Joel, & Cañete, 2009; Castilla & Fereres, 1990), unitless
s	0.041	Slope of saturation vapour pressure curve, kPa C^{-1}
R_n	0 or 0.000045	Net radiation at crop surface, measured at 0 with grow light off and 4.5 x 10^{-5} with grow light on, MJ $m^{-2}h^{-1}$
VPD	Variable	Measured hourly vapour pressure deficit, kPa
ρ	1.2	Mean atmospheric density, kg m^{-3}
r_R	Variable	Radiative resistance s m^{-1}
r_a	432	Aerodynamic external resistance, s m^{-1}

The Stanghellini equation estimates the potential evapotranspiration, ET_p. To determine the crop evapotranspiration ET_c, potential evapotranspiration is multiplied by a crop coefficient K_c (Equation 2).

$$ET_c = ET_p \times K_c \quad (2)$$

To then acquire an estimated amount of water used by the crop WU_e, the crop evapotranspiration must be multiplied by the crop area A_c, as defined in Equation 3.

$$WU_e = ET_c \times A_c \quad (3)$$

3 Results and discussion

3.1 Humidity addition via evapotranspiration in the bench scale greenhouse

Table 2 shows the estimated crop water use (WU_e) from the Stanghellini equation in g h^{-1} compared with the measured values WU_r. The crop water use corresponds directly with the expected increase in humidity in the controlled environment, as water taken up by plant roots is transpired via the leaves. The measured crop water use was slightly more than that calculated for all three experimental sets (+2.5%, +1.1%, and +2.3%), but falls within the standard error of the mean. The higher measured crop water use may also be accounted for by the fact that some irrigation water was not transpired, but was retained within plant tissue.

Table 2 Stanghellini equation output, including minimum, maximum, average, and standard error of the mean at different desiccant pumping velocities. In addition, the actual recorded crop water use is shown.

	Test 1: 2.3 cm s^{-1}				Test 2: 4.7 cm s^{-1}				Test 3: 8.1 cm s^{-1}				
Variable	**Min**	**Max**	**Avg**	**Std Err Mean**	**Min**	**Max**	**Avg**	**Std Err Mean**	**Min**	**Max**	**Avg**	**Std Err Mean**	**Description**
Et_p	0.02	0.28	0.08	0.00	0.03	0.27	0.11	0.00	0.04	0.28	0.13	0.00	Estimated ET by Stanghellini eq., mm h^{-1}
Et_c	0.01	0.17	0.05	0.00	0.02	0.16	0.07	0.00	0.02	0.17	0.08	0.00	Estimated hourly crop ET, mm h^{-1}
A_c	700	700	700	0	400	400	400	0	340	340	340	0	Recorded crop area, cm^2
WU_e	0.78	11.84	3.53	0.10	0.62	6.58	2.61	0.06	0.72	5.63	2.60	0.06	Estimated ET in g h^{-1}
WU_r	-	-	3.62	-	-	-	2.64	-	-	-	2.66	-	Actual recorded crop water use in g h^{-1}

3.2 **Humidity removal via liquid desiccants inside the membrane array**

The rate of rise in humidity was successfully slowed within the bench scale greenhouse air using the liquid desiccants inside the hydrophobic hollow fibre membrane array. Indoor relative humidity levels were kept from reaching saturation (100% relative humidity) and generally within the target humidity range (~70-90% relative humidity at ~23°C) for a longer period of time when compared to the control by the liquid desiccants (see Figure 3). The relative humidity in the indoor environment varied dynamically based upon the rate of evapotranspiration,

dehumidification and air temperature. In general, relative humidity of the indoor environment was higher during the “day” (light on, higher temperatures, more evapotranspiration, for 16 hours) vs. the “night” (light off, lower temperatures, less evapotranspiration, for 8 hours). The rate of dehumidification varied dynamically based upon the vapour pressure difference between the air and the desiccant. The vapour pressure difference between the desiccant and air is larger during the day, driving a higher humidity mass flow rate into the desiccant solution. The peak indoor humidity experienced during a day or night phase was limited by the evapotranspiration from the crop, the membrane surface area, the temperatures of the air and desiccant, and the concentration of the desiccant solution.

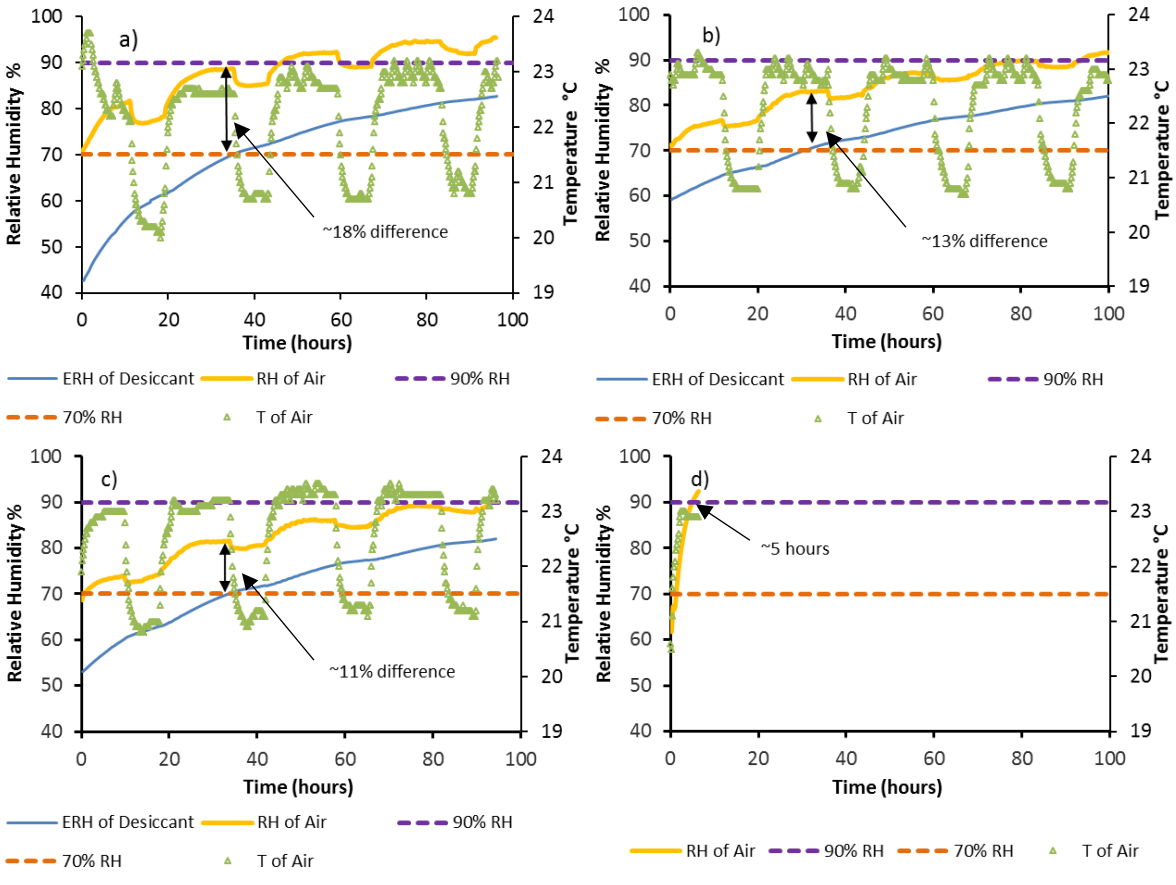

Figure 3 Recorded variations in temperature (T) and relative humidity (RH) of indoor air plotted against the equilibrium relative humidity (ERH) of the desiccant solution during a) Trial 1 at 2.3 cm s^{-1} b) Trial 2 at 4.7 cm s^{-1} and c) Trial 3 at 8.1 cm s^{-1} d) Trial 4 control with no liquid desiccant pumped through hollow fibres. The difference between the RH of the air and ERH of the desiccant when the desiccant is at 70% ERH is also pointed out at 18% in Trial 1, 13% in Trial 2, and 11% in Trial 3. In Trial 4, the time to reach 90% RH is noted as 5 hours.

Three experimental trial sets were conducted, each with a different desiccant flow rate/velocity through the hollow fibres. Trial 1, 2, and 3 velocities were 2.3 cm s^{-1}, 4.7 cm s^{-1}, and 8.1 cm s^{-1}, respectively. Figure 3 shows how the equilibrium relative humidity (ERH) of the desiccant varied against the relative humidity (RH) and temperature of the air. At the ERH, the vapour pressure of the desiccant is equal to the vapour pressure of humid air at the same temperature and relative humidity. In other words, the ERH is the minimum relative humidity to which the air at the same

326 temperature can be dried in contact with the liquid desiccant. ERH can be calculated when the
327 concentration by wt% of a liquid desiccant salt in solution is known (Davies & Knowles, 2006). In
328 a static system, the ERH of the desiccant and the RH of the air would be expected to come to
329 equilibrium. In the dynamic system, however, the RH of the air is continuously elevated by the
330 evapotranspiration from the crops. The extent to which the RH is elevated above the level of
331 the ERH of the desiccant is determined both by the transpiration rate of the plants and the
332 dehumidification rate into the desiccant.

333 The difference between the plotted ERH of the desiccant and the RH of the air was higher at the
334 slower solution velocities. When the ERH of the desiccant solution was equal to 70%, the RH of
335 the air was ~18% higher for solution velocity 2.3 cm s^{-1}, ~13% higher for solution velocity 4.7 cm
336 s^{-1}, and ~11% higher for solution velocity 8.1 cm s^{-1}. The faster velocity of the desiccant solution
337 corresponded to a smaller gap between the desiccant ERH and the air RH. It is suspected that
338 the reason for this difference is the change in the ERH of the desiccant from entry to exit of the
339 hollow fibres. The ERH plotted in Figure 3 is the ERH of the bulk desiccant solution in the tank,
340 not the instantaneous ERH of the desiccant in the hollow fibres. The ERH of the desiccant in the
341 hollow fibres would be expected to increase above that of the bulk solution as humidity is
342 absorbed, diluting the desiccant in the dynamic setting. Slower solution velocities correspond to
343 a longer hydraulic retention time of the desiccant in the hollow fibre, allowing more time for
344 dilution with a corresponding higher ERH at the exit from the hollow fibre.

345 In addition, the control for the experiment with no desiccant pumped through the hollow fibres
346 is shown in Figure 3d. In this case, the relative humidity in the controlled environment increases

above 90% after only 5 hours, as compared with a run time of ~100 hours for the desiccant dehumidification experiments.

Figure 4 shows how the calculated evapotranspiration compared to the measured dehumidification mass flow rate in g h^{-1} for each experimental trial. Evapotranspiration mass flow rates tended to be higher than the dehumidification rates during day phases at the early low indoor humidity levels. During later day phases with higher humidity, evapotranspiration rates approached a dynamic equilibrium with dehumidification rates. Evapotranspiration rates during night phases nearly equalled or fell below dehumidification rates. These results are expected, as lower humidity and higher solar radiation drive higher evapotranspiration. When humidity levels increase and/or solar radiation decreases, the evapotranspiration rate decreases. The increase in humidity therefore explains the decrease in evapotranspiration observed from the beginning to the end of each experimental run. From the desiccant side, dehumidification rates vary based upon the relative humidity due to vapour pressure difference.

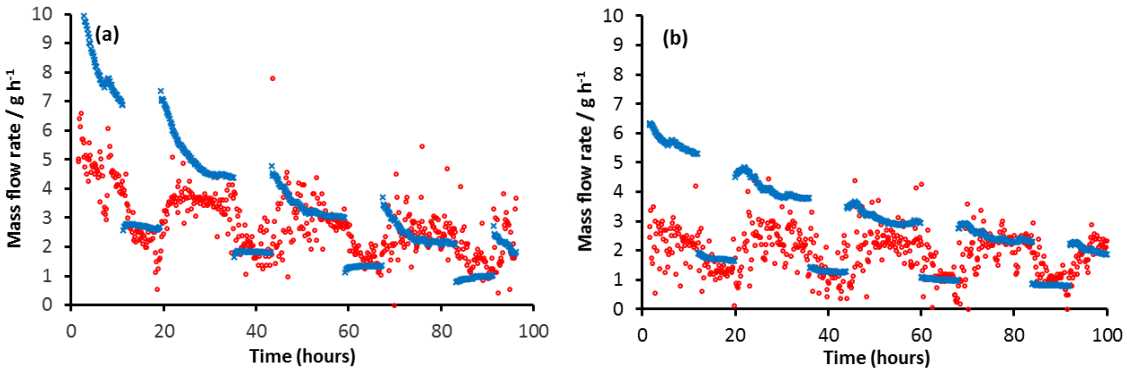

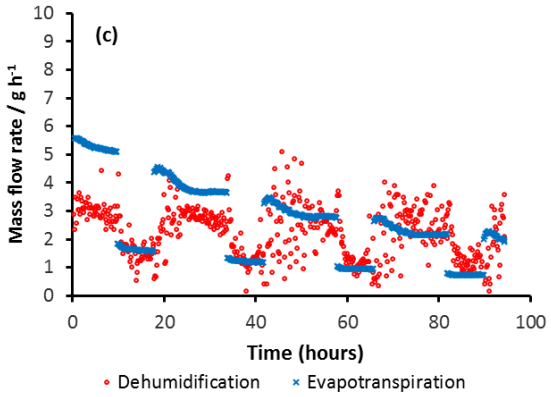

Figure 4 Mass flow rate of water vapour via evapotranspiration and dehumidification during a) Trial 1 at 2.3 cm s^{-1} b) Trial 2 at 4.7 cm s^{-1} and c) Trial 3 at 8.1 cm s^{-1}.

Figure 5 shows how the vapour pressure of the air, the vapour pressure of the bulk desiccant solution, and the vapour pressure difference between the two varied dynamically in response to changes in temperature and plant transpiration between the day and night cycles. The vapour pressure of the air increases dramatically when the light is turned on, reaches a semi-plateau where the transpiration rate comes near to the dehumidification rate, decreases dramatically when the light is shut off, and then reaches a semi-plateau again. The transpiration rate of the plants is limited by the vapour pressure difference between the plants and the air, thus it becomes slower at higher vapour pressures. Meanwhile, the mass transfer of humidity into the desiccant increases as the vapour pressure difference increases. Eventually the two rates come to a sort of dynamic equilibrium and a semi-plateau in vapour pressure is reached.

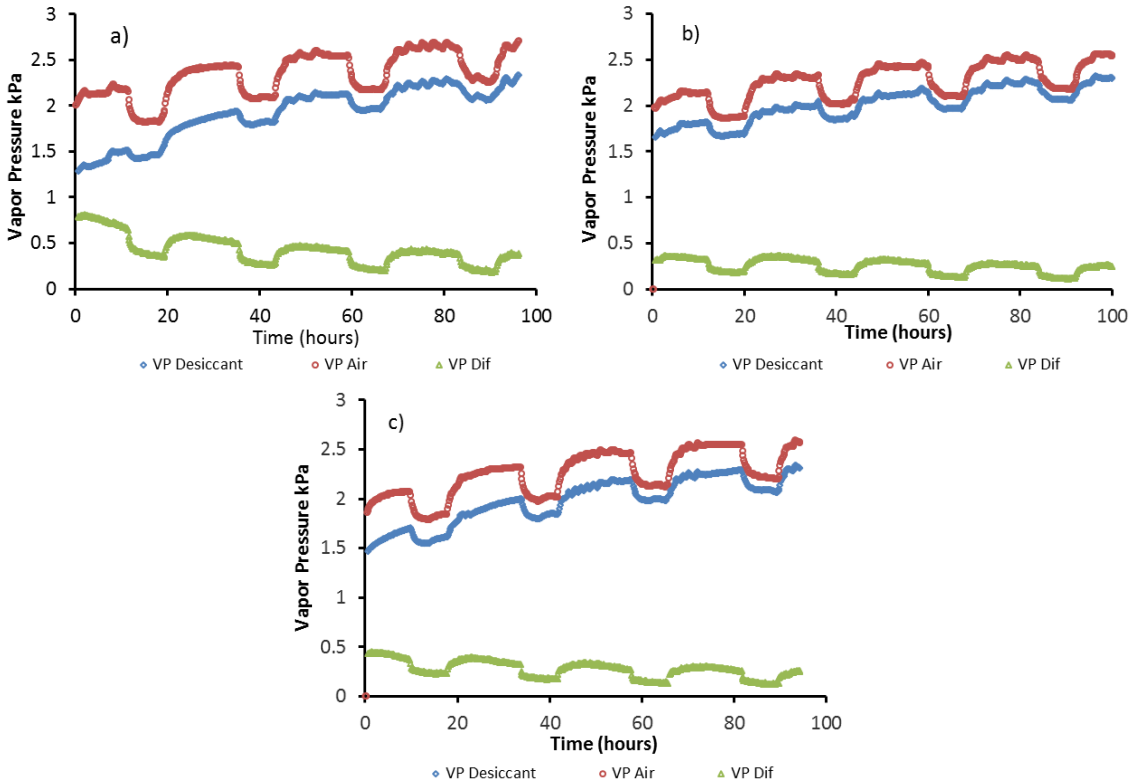

Figure 5 Recorded variations in vapour pressure (VP) of indoor air plotted against the VP of the desiccant solution and the vapour pressure difference (VP Dif) during a) Trial 1 at 2.3 cm s^{-1} b) Trial 2 at 4.7 cm s^{-1} and c) Trial 3 at 8.1 cm s^{-1}.

The average membrane vapour permeance normalized for vapour pressure and standard deviation increased from 0.27 g m^{-2} h^{-1} Pa^{-1} at a desiccant flow velocity of 2.3 cm s^{-1}, to 0.30 g m^{-2} h^{-1} Pa^{-1} at a desiccant flow velocity of 4.7 cm s^{-1}, and to 0.32 g m^{-2} h^{-1} Pa^{-1} at a desiccant flow velocity of 8.1 cm s^{-1}. Although the average permeance trends up with an increase in the velocity of the desiccant through the hollow fibres, the standard deviation also trends up from 0.04 g m^{-2} h^{-1} Pa^{-1} at a desiccant flow velocity of 2.3 cm s^{-1}, to 0.07 g m^{-2} h^{-1} Pa^{-1} at a desiccant flow velocity of 4.7 cm s^{-1}, and to 0.10 g m^{-2} h^{-1} Pa^{-1} at a desiccant flow velocity of 8.1 cm s^{-1} such that the differences between the dehumidification permeance at the three solution velocities are not significant. It is also important to bear in mind that there is no independent data available to

allow association of any effects with flow rate, rather than the changing properties over time, etc. A set of randomized replicated trials would be needed for this purpose. The vapour permeance observed in this study is similar to the permeance obtained using liquid desiccants with triple-bore PVDF hollow fibres of ~0.25 g m^{-2} hr^{-1} Pa^{-1} (Bettahalli et al., 2016) and falls within the range of vapour permeance observed by others using liquid desiccants with hollow fibre membranes prepared from polyetherimide (PEI) coated with polydimethylsiloxane (PDMS) (0.13-0.64 g m^{-2} hr^{-1} Pa^{-1} (Kneifel et al., 2006)).

3.3 Liquid desiccant and water cycles

A VMD process with simulated solar thermal energy input was used to regenerate the liquid desiccant and to produce fresh water for the bench-scale crop irrigation. The VMD flux ranged from ~2.8 kg m^{-2} h^{-1} at ~43% ERH to ~7 kg m^{-2} h^{-1} at ~76% ERH at a desiccant temperature of 30 °C while applying vacuum to achieve 3 mbar absolute pressure on the air side of the membrane (Figure 6). For a complete discussion of the VMD process, see Lefers et. al. (2018). The recovered fresh water was used as make-up irrigation water in hydroponics while the concentrated liquid desiccant was reused for dehumidification. The conductivity of the recovered fresh water (distillate) reused for irrigation was < 18 µS cm^{-1}, and is considered of suitable quality for use in irrigated agriculture of even very salt sensitive crops (Ayers & Westcot, 1985). These results show at a small scale the promise for developing a large-scale CEAS where humidity is controlled, captured and reused with liquid desiccant based systems.

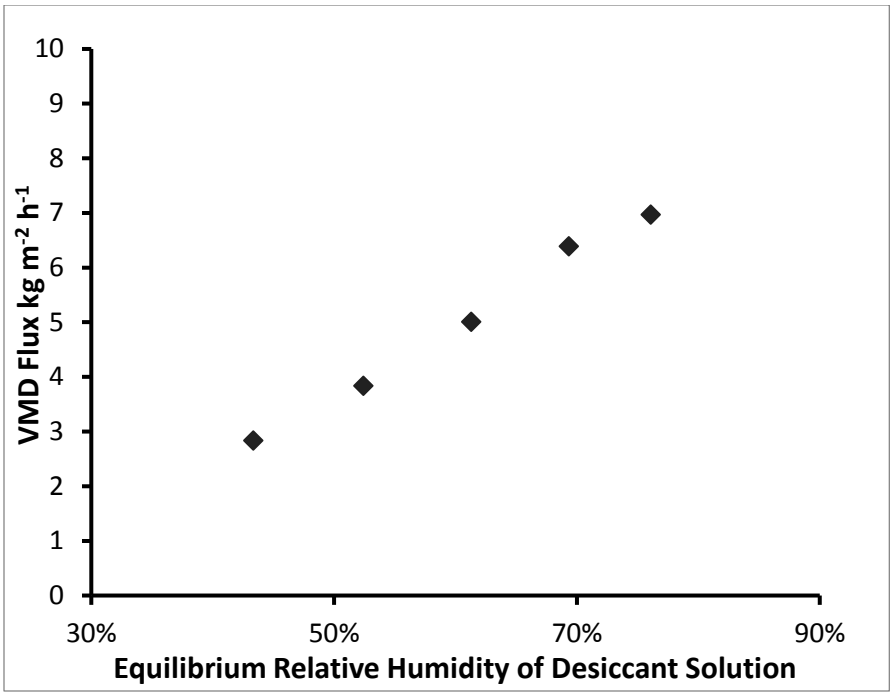

Figure 6 Vacuum membrane distillation flux of $MgCl_2$ desiccant solution as a function of ERH with desiccant at 30 °C and vacuum applied to reach 3 mbar of absolute pressure on the outer surface of the membrane

Anecdotally observed crop health and growth rate within the laboratory-scale CEAS was as expected for a hydroponic system of this size (very small). No adverse effects of the liquid desiccant dehumidification system were observed on the plants. On the contrary, the plants grew as desired. While anecdotal in nature, this observation confirms that the liquid desiccant dehumidification system can be used successfully with real crops.

The combined work has potential for greatly reducing the water footprint of CEA and also for reducing the air heating/cooling and dehumidification energy footprint of CEA. In addition, the proposed system has potential applications for totally closed CEAS in extreme environments, such as in outer space. If liquid desiccant humidity control and water cycling systems are combined with recycling hydroponics or aquaponics systems, the production water footprint of crops could be reduced to only the water that is actually retained within the plants and fruit. In

this case, the average production water footprint for a crop like tomatoes could be reduced from 171 L kg^{-1} (Mekonnen & Hoekstra, 2011) to ~1-2 L kg^{-1} of harvested fruit, providing a production water footprint reduction of ~99%.

3.4 Scale up implications

In a small commercial-sized CEA system, a peak humidity removal rate of ~3,000 kg day^{-1} (~125 kg hr^{-1}) would be required to maintain humidity at a set level for a 360 m^2 footprint greenhouse growing tomatoes at August conditions in Thuwal, Saudi Arabia (Lefers et al., 2016). To meet this dehumidification demand, approximately 1,250 m^2 of hollow fibre membrane surface area would be required at an expected vapour flux rate of 100 g m^{-2} hr^{-1} when the vapour pressure difference between the liquid desiccant and the air is kept at ~400 Pa (assuming a conservative flux of 0.25 g m^{-2} hr^{-1} Pa^{-1} for the PVDF hollow fibre membranes). This membrane surface area requirement corresponds to a total hollow fibre membrane length of ~219 km with a total volume of ~0.57 m^3 when utilizing the same triple-bore PVDF hollow fibres from the present study (1.82 mm outer diameter), about 0.0016 m^3 of membrane volume per m^2 of greenhouse area. Less total membrane area would be required for an application with less crop area (less transpiration), as might be expected in space travel or at the international space station.

As it relates to desiccant regeneration requirements, the VMD regeneration system must be sized to deliver the same or faster regeneration rate as compared to the expected humidity removal rate. In the above example, this rate must be greater than or equal to ~3,000 kg day^{-1}. A discussion of the VMD regenerator design is beyond the scope of this humidity control

manuscript, but details regarding design of such a system can be found in our other work (Lefers et al., 2018). If the regenerator is sized to deliver a regeneration rate much higher than the dehumidification rate, it can operate periodically rather than continuously. In this case, the total volume of the desiccant can be increased proportionally to the respective dehumidification and regeneration rates such that the vapour pressure of the desiccant is maintained at a desired level. A larger volume of desiccant absorbing the same amount of desiccant will not be diluted as quickly and will therefore require less frequent regeneration.

Many types of desiccants are available for use in such a system (Davies & Knowles, 2006; Greenspan, 1977; Lychnos et al., 2010; Wolf, 1966). For selection of a desiccant in scale up, there are a number of considerations to keep in mind. Among these considerations are cost, corrosivity, availability, health and safety, minimum ERH obtainable, volume of humidity that can be captured in a desired range per kg of salt, grower/designer preferences and experience, etc. Based upon this matrix, magnesium chloride was selected as the desiccant of choice in the present work; a different desiccant may be chosen for scale up based upon the same matrix.

4 Conclusions

A laboratory-scale liquid desiccant system utilizing an array of triple-bore hydrophobic hollow fibre membranes was tested for humidity control in CEA. The hollow fibre array was integrated into a bench-scale CEAS where transpired humidity from crop production was captured and removed from the closed indoor system by the liquid desiccant, controlling the humidity levels to maintain an environment optimal for plant growth. The relative humidity in the CEAS varied

dynamically based upon evapotranspiration of the crops and the rate of dehumidification. The average membrane vapour permeance rate varied from 0.26 to 0.31 g m^{-2} hr^{-1} Pa^{-1} at desiccant velocities through the hollow fibre lumens of 2.3 cm s^{-1} to 8.1 cm s^{-1}. Healthy plants were successfully grown and harvested in the CEAS with relative humidity levels generally controlled between 70-90% at ~23° C.

Acknowledgements

The research reported in this publication was supported by funding from King Abdullah University of Science and Technology (KAUST). The authors thank colleagues from Nanostructured Polymeric Membrane (NPM) group, as well as Water Desalination and Reuse Center (WDRC), and KAUST's Core Labs for their help on equipment and analysis. The graphical abstract and Figure 1 were produced by Xavier Pita, scientific illustrator at King Abdullah University of Science and Technology (KAUST). Philip Davies acknowledges granting of a Visiting Researcher position by KAUST.

References

Abdel-Salam, A. H., Ge, G. M., & Simonson, C. J. (2013). Performance analysis of a membrane liquid desiccant air-conditioning system. *Energy and Buildings, 62*(0), 559-569. doi: 10.1016/j.enbuild.2013.03.028

Albrecht, W., Kneifel, K., Weigel, T., Hilke, R., Just, R., Schossig, M., . . . Lendlein, A. (2005). Preparation of highly asymmetric hollow fiber membranes from poly(ether imide) by a modified dry–wet phase inversion technique using a triple spinneret. *Journal of Membrane Science, 262*(1–2), 69-80. doi: http://dx.doi.org/10.1016/j.memsci.2005.03.042

485 Alsaadi, A., Francis, L., Maab, H., Amy, G., & Ghaffour, N. (2014). Experimental and theoretical
486 analyses of temperature polarization effect in vacuum membrane distillation. *Journal of*
487 *Membrane Science, 471*, 138-148.

488 Alsaadi, A. S., Alpatova, A., Lee, J.-G., Francis, L., & Ghaffour, N. (2018). Flashed-feed VMD
489 configuration as a novel method for eliminating temperature polarization effect and
490 enhancing water vapor flux. *Journal of Membrane Science, 563*, 175-182.

491 Ayers, R. S., & Westcot, D. W. (1985). Water quality for agriculture Retrieved from
492 http://www.fao.org/docrep/003/T0234E/T0234E00.htm

493 Bakker, J. C. (1991). *Analysis of humidity effects on growth and production of glasshouse fruit*
494 *vegetables.* PhD, Wageningen Agricultural University, The Netherlands.

495 Bergero, S., & Chiari, A. (2010). Performance analysis of a liquid desiccant and membrane
496 contactor hybrid air-conditioning system. *Energy and Buildings, 42*(11), 1976-1986. doi:
497 10.1016/j.enbuild.2010.06.003

498 Bettahalli, N. M. S., Lefers, R., Fedoroff, N., Leiknes, T., & Nunes, S. P. (2016). Triple-bore hollow
499 fiber membrane contactor for liquid desiccant based air dehumidification. *Journal of*
500 *Membrane Science, 514*, 135-142. doi: 10.1016/j.memsci.2016.04.059

501 Campen, J. B., Bot, G. P. A., & de Zwart, H. F. (2003). Dehumidification of Greenhouses at
502 Northern Latitudes. *Biosystems Engineering, 86*(4), 487-493. doi:
503 https://doi.org/10.1016/j.biosystemseng.2003.08.008

504 Casanova, M. P., Messing, I., Joel, A., & Cañete, A. (2009). Methods to estimate lettuce
505 evapotranspiration in greenhouse conditions in the central zone of Chile. *Chilean Journal*
506 *of Agricultural Research, 69*(1), 60-70.

507 Castilla, N., & Fereres, E. (1990). The climate and water requirements of tomatoes in unheated
508 plastic greenhouses. *Agricoltura Mediterranea, 120*(3), 268-274.

509 Das, R. S., & Jain, S. (2013). Experimental performance of indirect air-liquid membrane contactors
510 for liquid desiccant cooling systems. *Energy, 57*(0), 319-325. doi:
511 10.1016/j.energy.2013.05.013

512 Das, R. S., & Jain, S. (2015). Performance characteristics of cross-flow membrane contactors for
513 liquid desiccant systems. *Applied Energy, 141*, 1-11. doi:
514 http://dx.doi.org/10.1016/j.apenergy.2014.12.014

515 Davies, P. A., & Knowles, P. R. (2006). Seawater bitterns as a source of liquid desiccant for use in
516 solar-cooled greenhouses. *Desalination, 196*(1-3), 266-279. doi:
517 10.1016/j.desa1.2006.03.010

Dean, J., Kozubal, E., Herrmann, L., Miller, J., Lowenstein, A., Barker, G., & Slayzak, S. (2012). *Solar-powered, liquid desiccant air conditioner for low-electricity humidity control*. (NREL/TP-7A40-56437). U.S. Department of Energy Retrieved from www.osti.gov/bridge.

Dijkink, B. H., Tomassen, M. M., Willemsen, J. H. A., & van Doorn, W. G. (2004). Humidity control during bell pepper storage, using a hollow fiber membrane contactor system. *Postharvest Biology and Technology, 32*(3), 311-320. doi: 10.1016/j.postharvbio.2003.12.002

FAO. (2016). Aquastat website Retrieved 2018/10/04

Fortunato, L., Jang, Y., Lee, J.-G., Jeong, S., Lee, S., Leiknes, T., & Ghaffour, N. (2018). Fouling development in direct contact membrane distillation: Non-invasive monitoring and destructive analysis. *Water Research, 132*, 34-41. doi: https://doi.org/10.1016/j.watres.2017.12.059

Gabelman, A., & Hwang, S.-T. (1999). Hollow fiber membrane contactors. *Journal of Membrane Science, 159*(1–2), 61-106. doi: http://dx.doi.org/10.1016/S0376-7388(99)00040-X

Greenspan, L. (1977). Humidity Fixed Points of Binary Saturated Aqueous Solutions. *Journal of Research of the National Bureau of Standards - A. Physics and Chemistry, 81A*(1), 89-96. doi: 10.6028/jres.081A.011

Hand, D. W. (1988). Effects of Atmospheric Humidity on Greenhouse Crops. *Acta Horticulturae, 229*, 143-158.

Hickman, G. W. (2014). *Commercial Greenhouse Vegetable Production Handbook for Temperate Regions*. Mariposa, CA, USA: Cuesta Roble (Oak Hill) Consulting.

Hwang, Y. H., Radermacher, R., Al Alili, A., & Kubo, I. (2008). Review of solar cooling technologies. *Hvac&R Research, 14*(3), 507-528. doi: Doi 10.1080/10789669.2008.10391022

Ilahi, W. F. F. (2009). *Evapotranspiration Models in Greenhouse.* Master of Science in Agricultural and Bioresearch Engineering, Wageningen University, the Netherlands.

Isetti, C., Nannei, E., & Magrini, A. (1997). On the application of a membrane air-liquid contactor for air dehumidification. *Energy and Buildings, 25*(3), 185-193. doi: Doi 10.1016/S0378-7788(96)00993-0

Kassem, T. K., Alosaimy, A.S., Hamed, A.M., Fazian, M. (2013). Solar powered dehumidification systems using desert evaporative coolers: Review. *International Journal of Engineering and Advanced Technology, 3*(1), 115-128.

Keniar, K., Ghali, K., & Ghaddar, N. (2015). Study of solar regenerated membrane desiccant system to control humidity and decrease energy consumption in office spaces. *Applied Energy, 138*, 121-132. doi: http://dx.doi.org/10.1016/j.apenergy.2014.10.071

551 Khan, A. Y. (1994). Sensitivity Analysis and Component Modeling of a Packed-Type Liquid
552 Desiccant System at Partial Load Operating-Conditions. *International Journal of Energy*
553 *Research, 18*(7), 643-655. doi: DOI 10.1002/er.4440180703

554 Kneifel, K., Nowak, S., Albrecht, W., Hilke, R., Just, R., & Peinemann, K. V. (2006). Hollow fiber
555 membrane contactor for air humidity control: Modules and membranes. *Journal of*
556 *Membrane Science, 276*(1-2), 241-251. doi: 10.1016/j.memsci.2005.09.052

557 Kozubal, E., Woods, J., Burch, J., Boranian, A., & Merrigan, T. (2011). Desiccant Enhanced
558 Evaporative Air-Conditioning (DEVap): Evaluation of a New Concept in Ultra Efficient Air
559 Conditioning (U. S. D. o. Energy, Trans.): National Renewable Energy Laboratory.

560 Lefers, R., Bettahalli, N. M. S., Fedoroff, N., Nunes, S. P., & Leiknes, T. (2018). Vacuum membrane
561 distillation of liquid desiccants utilizing hollow fiber membranes. *Separation and*
562 *Purification Technology, 199*, 57-63. doi: https://doi.org/10.1016/j.seppur.2018.01.042

563 Lefers, R., Bettahalli, N. M. S., Nunes, S. P., Fedoroff, N., Davies, P. A., & Leiknes, T. (2016). Liquid
564 desiccant dehumidification and regeneration process to meet cooling and freshwater
565 needs of desert greenhouses. *Desalination and Water Treatment, 57*(48-49), 23430-
566 23442. doi: 10.1080/19443994.2016.1173383

567 Lefers, R., Maliva, R. G., & Missimer, T. M. (2015). Seeking a consensus: water management
568 principles from the monotheistic scriptures. *Water Policy, 17*(5), 984-1002. doi:
569 10.2166/wp.2015.165

570 Lowenstein, A. (2008). Review of Liquid Desiccant Technology for HVAC Applications. *Hvac&R*
571 *Research, 14*(6), 819-839. doi: Doi 10.1080/10789669.2008.10391042

572 Lychnos, G., Fletcher, J. P., & Davies, P. A. (2010). Properties of seawater bitterns with regard to
573 liquid-desiccant cooling. *Desalination, 250*(1), 172-178. doi:
574 http://dx.doi.org/10.1016/j.desal.2008.11.019

575 Mekonnen, M. M., & Hoekstra, A. Y. (2011). The green, blue and grey water footprint of crops
576 and derived crop products. *Hydrology and Earth System Sciences, 15*, 1577-1600. doi:
577 10.5194/hess-15-1577-2011

578 Mohammad, A. T., Mat, S. B., Sulaiman, M. Y., Sopian, K., & Al-Abidi, A. A. (2013). Historical review
579 of liquid desiccant evaporation cooling technology. *Energy and Buildings, 67*, 22-33.

580 Resh, H. M. (2013). *Hydroponic Food Production* (Seventh ed.). Boca Raton, FL: CRC Press, Taylor
581 & Francis Group.

582 Stanghellini, C. (1987). *Transpiration of greenhouse crops. An aid to climate mangement.* PhD,
583 Wageningen Agricultural University, The Netherlands.

584 Villarreal-Guerrero, F., Kacira, M., Fitz-Rodríguez, E., Kubota, C., Giacomelli, G. A., Linker, R., &
585 Arbel, A. (2012). Comparison of three evapotranspiration models for a greenhouse
586 cooling strategy with natural ventilation and variable high pressure fogging. *Scientia*
587 *Horticulturae, 134*(0), 210-221. doi: http://dx.doi.org/10.1016/j.scienta.2011.10.016

588 Vuscovich, M. (2001). *Desarrollo de un modelo para determinar evapotranspiracion en*
589 *invernaderos.* Master of Science. Master's, Universidad de Concepcion, Chillan, Chile.
590 Retrieved from
591 http://www.bibliodigital.udec.cl/sdx/UDEC4/tesis/2001/vuscovich_m/html/index-
592 frames.html

593 Wolf, A. (1966). *Aqueous Solutions and Body Fluids; Their Concentrative Properties and*
594 *Conversion Tables*. New York: Hoeber Medical Division, Harper & Row.

595 Xu, J., Singh, Y. B., Amy, G. L., & Ghaffour, N. (2016). Effect of operating parameters and
596 membrane characteristics on air gap membrane distillation performance for the
597 treatment of highly saline water. *Journal of Membrane Science, 512*, 73-82.

598 Zhang, L. Z. (2011). An Analytical Solution to Heat and Mass Transfer in Hollow Fiber Membrane
599 Contactors for Liquid Desiccant Air Dehumidification. *Journal of Heat Transfer-*
600 *Transactions of the Asme, 133*(9).

601 Zhang, N., Yin, S.-Y., & Zhang, L.-Z. (2016). Performance study of a heat pump driven and hollow
602 fiber membrane-based two-stage liquid desiccant air dehumidification system. *Applied*
603 *Energy, 179*, 727-737. doi: https://doi.org/10.1016/j.apenergy.2016.07.037

604 Zhang, N., Zhang, L.-Z., & Xu, J.-C. (2016). A heat pump driven and hollow fiber membrane-based
605 liquid desiccant air dehumidification system: A transient performance study.
606 *International Journal of Refrigeration, 67*, 143-156. doi:
607 http://dx.doi.org/10.1016/j.ijrefrig.2016.01.001

608